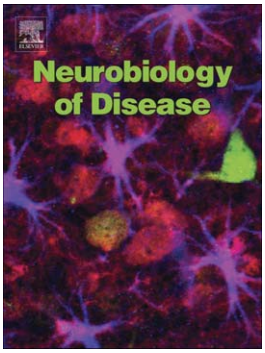

Loss of dopaminergic neurons and resulting behavioral deficits in mouse model of Angelman syndrome

Shalaka A. Mulherkar, Nihar Ranjan Jana

PII: S0969-9961(10)00254-8
DOI: doi: 10.1016/j.nbd.2010.08.002
Reference: YNBDI 2216

To appear in: *Neurobiology of Disease*

Received date: 21 February 2010
Revised date: 16 July 2010
Accepted date: 1 August 2010

Please cite this article as: Mulherkar, Shalaka A., Jana, Nihar Ranjan, Loss of dopaminergic neurons and resulting behavioral deficits in mouse model of Angelman syndrome, *Neurobiology of Disease* (2010), doi: 10.1016/j.nbd.2010.08.002

Loss of dopaminergic neurons and resulting behavioral deficits in mouse model of Angelman syndrome

Shalaka A. Mulherkar and Nihar Ranjan Jana*

Cellular and Molecular Neuroscience Laboratory, National Brain Research Centre, Manesar, Gurgaon - 122 050, India

*Address correspondence to:

Nihar Ranjan Jana,

Cellular and Molecular Neuroscience Laboratory,

National Brain Research Centre, Manesar, Gurgaon - 122 050, India

Tel: +91-124-2338922, Fax: +91-124-2338910,

e-mail: nihar@nbrc.ac.in

Abbreviations used: E6-AP, E6 associated protein; AS, Angelman syndrome; PD, Parkinson disease; PBS, phosphate-buffered saline; TH, tyrosine hydroxylase; DAT, dopamine transporter; GDNF, glial cell line-derived neurotrophic factor; DAPI, 4′,6-diamidino-2-phenylindole; PSD95, postsynaptic density 95.

Abstract

E6 associated protein is an E3 ubiquitin ligase encoded by the gene *Ube3a*. Deletion or loss of function of the maternally inherited allele of *Ube3a* leads to Angelman syndrome. In the present study, we show that maternal loss of *Ube3a* (*Ube3a*$^{m-/p+}$) in the mouse model leads to motor deficits that could be attributed to the dysfunction of the nigrostriatal pathway. The number of tyrosine hydroxylase positive neurons in the substantia nigra was significantly reduced in *Ube3a*$^{m-/p+}$ mice as compared to the wild type counterparts. The *Ube3a*$^{m-/p+}$ mice performed poorly in behavioral paradigms sensitive to nigrostriatal dysfunction. Even though the tyrosine hydroxylase staining was apparently same in the striatum of both genotypes, the presynaptic and postsynaptic proteins were significantly reduced in *Ube3a*$^{m-/p+}$ mice. These findings suggest that the abnormality in the nigrostriatal pathway along with the cerebellum produces the observed motor dysfunctions in *Ube3a*$^{m-/p+}$ mice.

Keywords: *Ube3a*, E6-AP, Angelman syndrome, nigrostriatal dysfunction, motor deficits

1. Introduction

The gene product of *Ube3a* called E6 associated protein (E6-AP) belongs to the HECT (Homologous to E6-AP C-terminus) domain family of E3 ubiquitin ligases. E6-AP, the best characterized protein in this family, tags ubiquitin molecules to proteins that are destined to be degraded through the proteasome (Mishra et al., 2009; Mishra and Jana, 2008; Scheffner et al., 1993; Wang and Pickart, 2005). Loss of function mutations or deletions of maternal *Ube3a* is known to cause Angelman syndrome (AS) (Fang et al., 1999; Kishino et al., 1997). Characteristics of the syndrome include motor dysfunction, seizures and mental retardation (Clayton-Smith and Laan, 2003). In the brain, the maternal allele of *Ube3a* is predominantly expressed as a result of tissue specific imprinting. Mature neurons exhibit maternal allele-specific expression (Albrecht et al., 1997; Rougeulle et al., 1997) although traces of paternal allele-specific expression are also detected. Biallelic expression is restricted to GFAP positive cells lining the ventricles and absent from GFAP positive astrocytes in other regions of the brain. In the brain, *Ube3a* predominantly expresses in the cerebellar Purkinje cells, neurons in the hippocampus, the cortex and substantia nigra (Dindot et al., 2008; Gustin et al., 2010). At the cellular level, E6-AP is localized in the nucleus as well as in the cytoplasm. Expression of E6-AP was also found in both presynaptic and postsynaptic compartments in cultured of hippocampal neurons (Dindot et al., 2008). *Ube3a* maternal deficient mice ($Ube3a^{m-/p+}$) exhibit learning and memory deficits as well as motor abnormalities (Heck et al., 2008; Jiang et al., 1998). The motor abnormalities in these $Ube3a^{m-/p+}$ mice are so far been shown due to dysfunction of the cerebellum. Paternal deficient *Ube3a* mice ($Ube3a^{m+/p-}$) fail to show these typical characteristics (Jiang et al., 1998).

The protective effect of *Ube3a*/E6-AP in neurodegenerative diseases was first showed by Cummings et al (Cummings et al., 1999). Spinocerebellar ataxia 1 (SCA1) is a polyglutamine disease in which the protein ataxin 1 undergoes aggregation and accumulates mostly in the nucleus. Loss of E6-AP in SCA1 transgenic mice remarkably limited the formation of nuclear inclusions in Purkinje cells of the cerebellum. However the pathology is exacerbated due to the toxic substrates of E6-AP that are accumulated in its absence (Cummings et al., 1999). Later, various studies showed that E6-AP degrades a number of misfolded proteins like polyglutamine, CFTR and α synuclein (Mishra et al., 2008; Mishra et al., 2009; Mulherkar et al., 2009) indicating that E6-AP probably functions as cellular quality control ubiquitin ligase.

Patients with AS have been shown to manifest typical features of Parkinson disease (PD) like tremors, cogwheel rigidity and bradykinesia. This condition was responsive to levodopa, which is widely used for the symptomatic treatment of PD (Harbord, 2001). Recently, we have demonstrated that E6-AP localizes to the Lewy bodies in PD brain and enhances the degradation of α synuclein, which is the main component of the Lewy bodies (Mulherkar et al., 2009). All these findings suggest a role of E6-AP in proper functioning of the dopaminergic system in the brain. In the present study, we report the effect of maternal loss of *Ube3a* on dopaminergic neurons in the substantia nigra. We observed that *Ube3a*$^{m-/p+}$ mice showed reduced number of dopaminergic neurons in the substantia nigra accompanied by poor performance in behavioural paradigms sensitive to nigrostriatal dysfunction.

2. Materials and methods

2.1. Materials

Mouse monoclonal anti-E6-AP antibody was purchased from BD Biosciences (San Jose, CA, USA). Rabbit polyclonal anti-E6-AP, anti-p53 and anti-GAPDH were purchased from Santa Cruz Biotechnologies (CA, USA). Rabbit polyclonal anti-tyrosine hydroxylase (TH) and anti-dopamine transporter (DAT) were purchased from Chemicon (Temecula, California, USA). Mouse monoclonal anti-synaptophysin from Sigma (St. Louis, MO, USA) and anti-PSD-95 from Stressgen (Victoria, Canada) were used. Anti-phospho Thr286 αCaMKII and anti-total α-CaMKII antibodies were from Santa Cruz Biotechnologies. Anti-mouse IgG-FITC, AP-conjugated anti-rabbit IgG, biotinylated anti-rabbit and anti-mouse IgG, HRP conjugated anti-rabbit IgG, VECTASTAIN-Elite ABC reagent and Novared staining kit were purchased from Vector Laboratories (Burlingame, CA, USA). Alexa flour 594 was purchased from Molecular probes (Eugene, OR, USA). All other chemicals unless mentioned were purchased from Sigma.

2.2. Animals

Heterozygous *Ube3a* mice were purchased from Jackson Laboratory (Jackson code: 129-*Ube3a*tm1Alb/J) and maintained in C57BL/6 background. The genotyping was carried out using PCR as described previously ((Jiang et al., 1998). Different crosses of mice were used to get either maternal deficient or paternal deficient mice as described earlier (Jiang et al., 1998). Mice used in all the experiments were 7-8 month old males. Animals had access to pelleted diet and water *ad libitum*. All animal experiments were carried out as per the institutional guidelines for the use and care of animals. All efforts were made to minimize animal suffering and to reduce the number of animals used.

2.3. Behavioral tests

Gait analysis. For footprint gait analysis, the hind-paws of the mice were dipped in red nontoxic paint, and they were placed at an open end of a wooden tunnel (40 cm x 5 cm) lined with paper. The mice were trained for 2 days to walk through the tunnel and then tested for two trials. Two to four steps from the middle portion of each run were measured for hind-stride length, hind-base width (the distance between the right and left hind-limb strides).

Rotarod test. Mice were placed on the rotarod (Scientific Instruments, New Delhi) and initially trained to stay on the constant speed of 5 rpm. Mice that would fall were repeatedly placed back on the rod until they were able to stay on the rotarod for at least 30 s. Mice were trained for 2 days before the test and then tested for four trials per day for 5 days with the maximum speed reaching 25 rpm. The latency to fall was recorded for each trial, and the average of four trials was reported. All trials were terminated at 150 s.

Balance beam task. Mice were trained to cross a 20 mm wide, 80 cm long beam, which was elevated 50 cm above base level. A dark box was kept at the opposite end of the beam. Traversal time and number of slips were measured as mice traversed the beam. Time when mouse stopped for apparent olfactory cues was not included. After training with a 20 mm diameter square beam, mice were additionally tested using square (8 and 12 mm diameter) and round (8, 12 and 20 mm diameter) beams. All square beams were used on day 1 of testing while all round beams were used the next day. Mice were trained for 2 days before the test and then tested for 3 trials on the same day. Mean values were used for statistical analysis.

Clasping behaviour. Mice were suspended by their tails. The time for which the mice clasped their hind limbs was recorded. The time was then scored as follows: 4, 15-30 s; 3, 10-15 s; 2, 5-10 s; 1, 0-5 s and 0, 0 s.

Pole test. The pole test was performed as described earlier (Matsuura et al., 1997). Briefly, prior to testing, mice were acclimated to a 50 cm tall, cloth-wrapped, 1.5 cm diameter pole. Animals were placed head upward on top of the pole. Both wild type and *Ube3a*$^{m-/p+}$ mice received 2 days of training that consisted of 3 trials for each session. On the test day, animals received 3 trials and total time to descend was measured. The mean of three trials was used for both the groups.

Adhesive removal test. Motor response to sensory stimuli was measured with the adhesive removal test as described earlier (Fleming et al., 2004). Small adhesive stimulus (one-quarter inch) was placed on the snout of the mouse, and the time to remove the stimulus was recorded. The animals would raise both forelimbs toward their face and swipe off the stimulus with both forepaws. Each animal received two trials, and each mouse had an inter trial interval of at least 2 min. All testing was performed in the animal's home cage, and cage mates were temporarily removed during testing. If the animal did not remove the stimulus within 60 s, the experimenter removed it, and the trial for the next mouse was initiated.

2.4. Immunostaining and stereological counting

Animals were anaesthetized and perfused transcardially with phosphate-buffered saline (PBS) followed by 4% paraformaldehyde (w/v) in PBS and postfixed in paraformaldehyde. The cryostat cut sections (20 μm thickness) were exposed to hydrogen peroxide (3% v/v) to block the endogenous peroxidase reaction, blocked with 3% BSA

and then incubated overnight with primary antibody. Sections were then washed, treated with biotinylated secondary IgG (diluted 1: 500 in PBS) for 2 h, washed and incubated with VECTASTAIN-Elite ABC reagent. The color was developed using Novared kit. The TH, DAT, symaptophysis and PSD95 antibodies were used in 1:800, 1:200, 1:500 and 1:250 dilutions respectively. For immunofluorescence staining the secondary antibodies used were conjugated with either Alexa flour 594 (dilution 1:1000) or FITC (dilution 1:500) and the sections were counterstained with DAPI. The number of TH positive neurons was counted stereologically as described earlier (Karunakaran et al., 2007). Cryostat-cut coronal sections (20 μm thickness) were prepared throughout the entire midbrain from a random start position, and every fifth section was processed for TH immunofluorescence staining. Sections were visualized after incubation with secondary antibody conjugated to Alexa fluor 594 under fluorescent microscope. The pars compacta region was delineated for stereological counting. The number of TH positive neurons in the substantia nigra pars compacta (SNpc) was counted. For quantification of immunohistochemical staining, the stained sections were observed under 4X magnification and the entire striatum was traced using the Neurolucida 7 software (MBF biosciences, Vermont, USA). Based on the grid, ten squares (10000 μm^2 area each) were randomly selected from the contoured striatal area. Both left and right striata were analyzed separately and two sections per brain were analyzed for a number of four animals in each group. All parameters were kept same for all the sections.

2.5. Immunoblotting

Mice were sacrificed by cervical dislocation, different parts of the brain were carefully removed and stored at −80°C. Brain samples were homogenized in lysis buffer

containing 20 mM Tris; pH 7.5, 1 mM EGTA, 1 mM EDTA, 1 mM Sodium pyrophosphate, 1 mM sodium orthovanadate, 1 mM sodium fluoride and protease inhibitor tablet (Roche Diagnostics, India), centrifuged at 10,000 x g for 15 min and the supernatants were collected at stored at −80°C. The supernatants were then run on a 10% SDS-PAGE followed by immunoblot analysis as previously described (Mulherkar et al., 2009).

2.6. Statistical analysis

Statistical analysis of the data was performed using either one-way or two-way analysis of variance. The Student Newman Kuell's test was conducted to compare individual means where analysis of variance indicated statistical differences. The level of significance for all analysis was set at $p<0.05$.

3. Results

3.1. Motor impairments in Ube3a$^{m-/p+}$ mice

In order to check for the motor deficits caused due to loss of maternal *Ube3a*, we performed various behavioural tests on 7-8 months old mice. The gait analysis of mice revealed significantly longer hind limb stride length in the *Ube3a*$^{m-/p+}$ mice compared to the wild type (*Ube3a*$^{m+/p+}$) (Fig.1A). There was no significant difference in the hind base width between the two genotypes. Our findings are very similar with the observations made by Heck et al (Heck et al., 2008), however, hind limb stride length seems to be much longer in our older mice. To assess motor coordination we tested the mice on rotarod. *Ube3a*$^{m-/p+}$mice had significantly shorter latency to fall than both *Ube3a*$^{m+/p+}$ and *Ube3a*$^{m+/p-}$ mice (Fig. 1B). Rotarod test results were also in accordance with previous reports (Heck et al., 2008; Jiang et al., 1998). However, rotarod performances were also

comparatively very poor in the older *Ube3a*$^{m-/p+}$mice. We next analyzed the fine motor skills of these mutant mice using balance beam test. *Ube3a*$^{m-/p+}$ mice took longer time to cross the square beams and as the difficulty level increased (width of the beam decreased), there was significant difference between the time taken by *Ube3a*$^{m-/p+}$ and *Ube3a*$^{m+/p+}$ mice. Similar kinds of results were obtained when mice were allowed to cross round beam (Fig. 1C and 1D). The maternal deficient *Ube3a* mice showed significantly more number of hind limb slips than the wild type mice on both square and round beams (Fig. 1E and 1F). The mutant mice also showed hind limb clasping which is a sign of basal ganglia dysfunction (Fig.2A). The *Ube3a*$^{m-/p+}$ mice showed significantly longer clasping duration (clasping score 2.25 ± 0.629; n=6) while the wild type mice did not exhibit clasping at all. The mice were further subjected to the test that was designed to assess the nigrostriatal deficits. The time taken by the mice to descend a vertical pole in the pole test was recorded (Fig.2B). The latency to climb downwards was significantly more in *Ube3a*$^{m-/p+}$ than the wild type mice. We then tested the mice for adhesive removal test, which is a sensorimotor test sensitive to dopamine and found that *Ube3a*$^{m-/p+}$ mice took significantly longer time to remove the adhesive attached to the snout than the wild type mice (Fig. 2B).

3.2. Decreased number of TH positive neurons in the substantia nigra of Ube3a$^{m-/p+}$ *mice.*

Since the behavioural deficits were related to the nigrostriatal dysfunction in mice, we looked at the dopaminergic system in the midbrain. Mice were sacrificed and brain samples were collected for immunohistochemistry. The sections were double immunostained with TH and E6-AP antibodies. As shown in figure 3A, majority of TH

positive dopaminergic neurons in the substantia nigra expressed E6-AP that was absent in the *Ube3a*$^{m-/p+}$ mice indicating the imprinted expression of E6-AP in dopaminergic neurons. We stereologically quantified the number of dopaminergic neurons in the substantia nigra of *Ube3a*$^{m-/p+}$ along with wild type mice and found that maternal deficient mice had significantly less number of dopaminergic neurons. (Fig.3B). The imprinted expression of E6-AP in the different parts of *Ube3a*$^{m-/p+}$ mice brain along with wild type counterpart is shown in supplementary figure S1.

We next detected TH and DAT levels in the striatum of both the genotypes using immunohistochemical staining and immunoblot analysis (Fig. 4). The TH levels did not alter among these genotypes however, DAT showed mild increase in its expression in the striatum of *Ube3a*$^{m-/p+}$mice (Fig 4 and Supplementary Fig.S2 for densitometric quantification data). The unaltered TH staining in the striatum of both genotypes suggest that the dopaminergic innervations were grossly similar. Since *Ube3a*$^{m-/p+}$ mice showed dysfunction in nigrostriatal dopaminergic pathway, we thought that dopamine release machinery might be affected in these mutant mice. Decreased dopamine levels in the striatum is known to increase the phosphorylation status of αCaMKII (Brown et al., 2005; Picconi et al., 2004). Therefore, we checked for the phosphorylation of αCaMKII as it is also known to be increased in the hippocampus of *Ube3a*$^{m-/p+}$ mice and involved in synaptic plasticity (Weeber et al., 2003). We have detected a significant increase (about 1.5-fold) in the levels of phospho Thr286 αCaMKII in the striatum of *Ube3a*$^{m-/p+}$ mice (Fig.4B and Supplementary Fig.S2B for densitometric quantitative analysis).

Next we studied the levels of various synaptic proteins in the striatum of these mice, as *Ube3a*/E6-AP is known to regulate synapse formation. Immunohistochemical

analysis for presynaptic protein synaptophysin and postsynaptic density protein PSD95 showed significant reduction in their amounts in the striatum of *Ube3a*$^{m-/p+}$ mice compared to the wild type mice (Fig.5A and Supplementary Fig.S3A for quantitative analysis data). Immunoblot analysis also demonstrated significantly decreased levels of both synaptophysin and PSD95 in the striatum of *Ube3a*-maternal deficient mice (Fig. 5B and Fig.S3B for quantitative analysis data).

4. **Discussion**

The well-studied dysfunctions in the motor behaviour of *Ube3a*$^{m-/p+}$ mice are until now reasoned to be due to loss of *Ube3a* in the cerebellum. We subjected these mice to a number of behavioural tests to further study these motor deficits. In the footprint gait analysis the increased stride length and wide hind base width indicate ataxic gait. The rotarod test showed that the *Ube3a*$^{m-/p+}$ mice performed poorly as compared to the wild type mice (*Ube3a*$^{m+/p-}$). These motor deficits seem to be more severe in our study of older *Ube3a*$^{m-/p+}$ mice than younger mice reported earlier (Heck et al., 2008; Jiang et al., 1998). However, the gait analysis and rotarod test assess general neurological deficit and do not reveal dysfunction in any particular areas of brain. We then used tests that detect changes in the nigrostriatal pathway. The balance beam test was originally designed to test ageing and dopaminergic function in rats (Drucker-Colin and Garcia-Hernandez, 1991) and has been used to show motor dysfunction in MPTP treated mice (Goldberg et al., 2003; Meredith and Kang, 2006; Quinn et al., 2007). The increased number of hind limb slips of *Ube3a*$^{m-/p+}$ mice in balance beam test reflects impaired motor coordination probably due to the dysfunction in nigrostriatal dopaminergic pathway.

The clasping behaviour is widely used to study the damage or dysfunction of the basal ganglia in mice (Tanaka et al., 2004). Although clasping is considered a feature of general neurological deficit, the striatal delivery of GDNF to Huntington's disease transgenic mice delayed the emergence of clasping (McBride et al., 2006). This means that clasping could demonstrate compromised basal ganglia. Hence, the test could be an assessment of the functioning of the basal ganglia. The wild type *Ube3a* $^{m+/p+}$ mice of the same age did not show clasping behaviour at all, while *Ube3a*$^{m-/p+}$ mice scored higher in the clasping score. The results of both pole test and adhesive removal test further indicate the dysfunction of nigrostraital dopaminergic system in *Ube3a*$^{m-/p+}$ mice. The pole test is a sensitive method to assess motor deficits caused by dopamine depletion (Chandran et al., 2008; Fleming et al., 2004; Kim et al., 2005; Matsuura et al., 1997). In the adhesive removal test, the animal has to use fine motor skills of the forepaw to remove the adhesive. This test is a sensorimotor test, which is sensitive to subtle losses of dopamine (Meredith and Kang, 2006).

Since behavioral studies suggested the dysfunction of nigrostriatal dopaminergic pathway, we further studied this pathway in detail. Stereological quantification of TH positive neurons in the substantia nigra showed significantly less number of neurons in the *Ube3a*$^{m-/p+}$ mice than their wild type counterpart. Lesser number of neurons could in turn affect the innervations to the striatum. In contrast, TH staining in the striatum showed no difference between the two genotypes. But the behavioral deficits observed suggested low dopamine levels and therefore an imbalance in the proper functioning of the striatum. E6-AP protein is known to be present in the synapses and influence experience dependent synaptic plasticity in the neocortex (Dindot et al., 2008; Yashiro et

al., 2009). So we looked at the synaptic vesicle proteins, as absence of E6-AP would have some effect on the synapses. Immunostaining with presynaptic protein synaptophysin and postsynaptic density protein PSD95 showed drastic reduction in their respective levels in the *Ube3a*$^{m-/p+}$mice. This could mean that the synaptic vesicular machinery is disturbed and either improper formation or maintenance of synapses leads to low dopamine levels. There could also be a problem with the storage or release of dopamine that ultimately leads to dysfunction of the nigrostriatal pathway. Studying the release and uptake rates of dopamine would bring out the exact step at which the pathway has failed.

It has been shown that *Ube3a*$^{m-/p+}$ mice have abnormal high levels of phospho αCaMKII in the hippocampus (Weeber et al., 2003). We found higher levels of phospho Thr286 αCaMKII in the striatum of *Ube3a*$^{m-/p+}$ mice than wild type. In an animal model of PD, the addition of the toxin 6-Hydroxydopamine (6-OHDA) in the striatum leads to depletion of dopamine, abnormal increase in phosphorylation of αCaMKII and subsequent deficits in motor function. L-DOPA reverses the increase in the levels of phospho αCaMKII and rescues the motor deficits (Brown et al., 2005; Picconi et al., 2004). The observed higher levels of phospho αCaMKII in the *Ube3a*$^{m-/p+}$ mice could be due to low level of dopamine that need further investigation. Our findings along with other (Harbord, 2001) strongly suggests L-DOPA therapy for symptomatic treatment of AS. Thus our data identify that maternal loss of *Ube3a*/E6-AP leads to dysfunction in the nigrostriatal pathway in addition to the cerebellar dysfunction, which is already been studied. The observed motor deficits are summation of more than one dysfunctional pathway.

Acknowledgements

This work was supported by the Department of Biotechnology, Government of India. S. M. was supported by research fellowship from the Council of Scientific and Industrial Research, Government of India. We thank Mr. M. Singh, Mr.Partha Dey and Mr. Narender for technical assistance. We thank Dr. Narender Dhingra from NBRC, India for anti-synaptophysin and anti-PSD95 antibodies and Dr. Shiv Kumar Sharma from NBRC, India for anti-phospho Thr 286 αCaMKII and anti-total αCaMKII antibodies.

References

Albrecht, U., et al., 1997. Imprinted expression of the murine Angelman syndrome gene, Ube3a, in hippocampal and Purkinje neurons. Nat Genet. 17**,** 75-78.

Brown, A., et al., 2005. Dopamine depletion alters phosphorylation of striatal proteins in a model of Parkinsonism. Eur J Neurosci. 22**,** 247-256.

Chandran, J. S., et al., 2008. Progressive behavioral deficits in DJ-1-deficient mice are associated with normal nigrostriatal function. Neurobiol Dis. 29**,** 505-14.

Clayton-Smith, J., Laan, L., 2003. Angelman syndrome: a review of the clinical and genetic aspects. J Med Genet. 40**,** 87-95.

Cummings, C. J., et al., 1999. Mutation of the E6-AP ubiquitin ligase reduces nuclear inclusion frequency while accelerating polyglutamine-induced pathology in SCA1 mice. Neuron. 24**,** 879-92.

Dindot, S. V., et al., 2008. The Angelman syndrome ubiquitin ligase localizes to the synapse and nucleus, and maternal deficiency results in abnormal dendritic spine morphology. Hum Mol Genet. 17**,** 111-18.

Drucker-Colin, R., Garcia-Hernandez, F., 1991. A new motor test sensitive to aging and dopaminergic function. J Neurosci Meth. 39**,** 153-61.

Fang, P., et al., 1999. The spectrum of mutations in UBE3A causing Angelman syndrome. Hum. Mol. Genet. 8**,** 129-35.

Fleming, S. M., et al., 2004. Early and progressive sensorimotor anomalies in mice overexpressing wild-type human alpha-synuclein. J Neurosci. 24**,** 9434-40.

Goldberg, M. S., et al., 2003. Parkin-deficient mice exhibit nigrostriatal deficits but not loss of dopaminergic neurons. J Biol Chem. 278**,** 43628-35.

Gustin, R. M., et al., 2010 Tissue-specific variation of Ube3a protein expression in rodents and in a mouse model of Angelman syndrome. Neurobiol Dis. doi:10,1016/jnbd2010.04.012.

Harbord, M., 2001. Levodopa responsive Parkinsonism in adults with Angelman Syndrome. J. Clin. Neurosci. . 8**,** 421-22.

Heck, D. H., et al., 2008. Analysis of cerebellar function in Ube3a-deficient mice reveals novel genotype-specific behaviors. Hum Mol Genet. 17**,** 2181-9.

Jiang, Y. H., et al., 1998. Mutation of the Angelman ubiquitin ligase in mice causes increased cytoplasmic p53 and deficits of contextual learning and long-term potentiation. Neuron. 21**,** 799-11.

Karunakaran, S., et al., 2007. Activation of apoptosis signal regulating kinase 1 (ASK1) and translocation of death-associated protein, Daxx, in substantia nigra pars compacta in a mouse model of Parkinson's disease: protection by alpha-lipoic acid. Faseb J. 21**,** 2226-36.

Kim, R. H., et al., 2005. Hypersensitivity of DJ-1-deficient mice to 1-methyl-4-phenyl-1,2,3,6-tetrahydropyrindine (MPTP) and oxidative stress. Proc. Natl. Acad. Sci. U S A. 102**,** 5215-20.

Kishino, T., et al., 1997. UBE3A/E6-AP mutations cause Angelman syndrome. Nat Genet. 15**,** 70-73.

Matsuura, K., et al., 1997. Pole test is a useful method for evaluating the mouse movement disorder caused by striatal dopamine depletion. J. Neurosci. Methods. 73**,** 45-48.

McBride, J. L., et al., 2006. Viral delivery of glial cell line-derived neurotrophic factor improves behavior and protects striatal neurons in a mouse model of Huntington's disease. Proc. Natl. Acad. Sci. U S A. 103**,** 9345–50.

Meredith, G. E., Kang, U. J., 2006. Behavioral Models of Parkinson's Disease in Rodents: A New Look at an Old Problem. Mov Disord. 21**,** 1595-06.

Mishra, A., et al., 2008. E6-AP promotes misfolded polyglutamine proteins for proteasomal degradation and suppresses polyglutamine protein aggregation and toxicity. J Biol Chem. 283**,** 7648-56.

Mishra, A., et al., 2009. The ubiquitin ligase E6-AP is induced and recruited to aggresomes in response to proteasome inhibition and may be involved in the ubiquitination of HSP70 bound misfolded proteins. J Biol Chem. 284, 10537-45.

Mishra, A., Jana, N. R., 2008. Regulation of turnover of tumor suppressor p53 and cell growth by E6-AP, a ubiquitin protein ligase mutated in Angelman mental retardation syndrome. Cell Mol Life Sci. 65**,** 656-66.

Mulherkar, S. A., et al., 2009. The ubiquitin ligase E6-AP promotes degradation of alpha-synuclein. J Neurochem. 110**,** 1955-64.

Picconi, B., et al., 2004. Abnormal Ca2+ -Calmodulin-Dependent Protein Kinase II Function Mediates Synaptic and Motor Deficits in Experimental Parkinsonism. J. Neurosci. 24**,** 5283-91.

Quinn, L. P., et al., 2007. A beam-walking apparatus to assess behavioural impairments in MPTP-treated mice: Pharmacological validation with R-(−)-deprenyl. J Neurosci Meth. 164**,** 43-49.

Rougeulle, C., et al., 1997. The Angelman syndrome candidate gene, UBE3A/E6-AP, is imprinted in brain. Nat Genet. 17**,** 14-15.

Scheffner, M., et al., 1993. The HPV-16 E6 and E6-AP complex functions as a ubiquitin-protein ligase in the ubiquitination of p53. Cell. 75**,** 495-5.

Tanaka, M., et al., 2004. Trehalose alleviates polyglutamine-mediated pathology in a model of Huntington disease. Nat. Med. 10**,** 148-54.

Wang, M., Pickart, C. M., 2005. Different HECT domain ubiquitin ligases employ distinct mechanisms of polyubiquitin chain synthesis. Embo J. 24**,** 4324-33.

Weeber, E. J., et al., 2003. Derangements of hippocampal calcium/calmodulin-dependent protein kinase II in a mouse model for Angelman mental retardation syndrome. J. Neurosci. 23**,** 2634-44.

Yashiro, K., et al., 2009. Ube3a is required for experience-dependent maturation of the neocortex. Nat Neurosci. 12**,** 777-83.

Figure legends

Fig.1. Motor deficits in *Ube3a*$^{m-/p+}$ mice.

A) Gait analysis. Hind paws of mice aged 7-8 months were dipped in nontoxic red paint. The footprint was analysed to calculate the stride length and hind base width. *Ube3a*$^{m-/p+}$ had significantly longer stride length than the *Ube3a*$^{m+/p+}$mice. There was no significant difference in the hind base width between the two genotypes. Data represented as mean ± SEM; (n=5). *p<0.05 with compared to wild type mice. B) Rotarod test. *Ube3a*$^{m-/p+}$ mice had significantly shorter latencies to stay on the rotating rod as compared to the *Ube3a*$^{m+/p+}$ or *Ube3a*$^{m+/p-}$ mice. The average of all the four trials on a single day across the animals were plotted as each data point. One-way ANOVA was used to analyze the data. Data represented as mean ± SEM; (n=5). *p<0.05 in comparison to the wild type and paternal deficient mice. C & D) Balance beam test. *Ube3a*$^{m-/p+}$ mice took significantly longer time to cross the 8 mm long square beam as well as round beam of 8 mm width than the *Ube3a*$^{m+/p+}$ mice. There was no significant difference in the time taken to cross beams of 20 mm and 12 mm width. Two-way ANOVA was used to analyze the data. Data represented as mean ± SEM; (n=5). *p<0.05 in comparison to the wild type mice. E & F) *Ube3a*$^{m-/p+}$ mice had more number of slips than the *Ube3a*$^{m+/p+}$ mice on the square beams as well as the round beams of different widths. The number of slips on all squere as well as round beams were significantly different between the two genotypes. Two-way ANOVA was used to analyze the data. Data represented as mean ± SEM; (n=5). *p<0.05 in comparison to the wild type mice.

Fig.2. Motor assessment sensitive to nigrostriatal dysfunction.

A) *Ube3a*$^{m-/p+}$ mice showed foot clasping behaviour while *Ube3a*$^{m+/p+}$ mice held their hind limbs outwards when suspended by the tail. The time for which the mice clasped their hind limbs was recorded. The time was then scored as follows: 4, 15-30 s; 3, 10-15 s; 2, 5-10 s; 1, 0-5 s and 0,0 s. *Ube3a*$^{m-/p+}$ mice showed clasping behaviour for longer duration (2.25 ± 0.629; *p< 0.01; n=6) while wild type mice did not exhibit clasping. B) Pole test and adhesive removal test. Mice were placed on a 50 cm vertical pole and the time taken to descend was recorded. *Ube3a*$^{m-/p+}$ mice took significantly longer to descend from the pole than the wild type mice. For adhesive removal test, small adhesive tape was put on the snout of the animals and the time to remove the tape was recorded. The *Ube3a*$^{m-/p+}$ mice took longer to remove the adhesive than the *Ube3a*$^{m+/p+}$ mice. Data represented as mean ± SEM; (n=6). *p<0.05 in comparison with the wild type mice.

Fig.3. Reduced number of TH positive neurons in the substantia nigra of *Ube3a*$^{m-/p+}$ mice.

A) Double immunolabeling of TH and E6-AP in the midbrain revealed that E6-AP expression was present in TH positive neurons in wild type *Ube3a*$^{m+/p+}$ mice while absent in the heterozygous *Ube3a*$^{m-/p+}$ mice. FITC-conjugated secondary was used to detect E6-AP and Alexa fluor 594 was used to detect TH. Scale bar represents 200 μm at 10X magnification (upper panel) and 50 μm at 40X magnification (lower panel). B) Stereological estimation revealed that the number of TH positive neurons in the substantia nigra of *Ube3a*$^{m-/p+}$ mice was significantly less than the number of neurons in the wild type mice. Data represented as mean ± SEM; (n=6). *p<0.05 in comparison to the wild type mice.

Fig.4. A) Representative immunohistochemical staining for TH and DAT in the striatum of the wild type and *Ube3a*-maternal deficient mice. Brain sections of 8 month old mice were used for staining. Scale bar represents 50 μm. B) Immunoblot analysis of phospho Thr^{286}αCaMKII, total αCaMKII, TH, DAT and GAPDH in the striatum of $Ube3a^{m-/p+}$ mice along with wild type. Each lane represent sample from different mice.

Fig.5. A) Representative immunohistochemical staining of synaptophysin and PSD95 in the striatum of the wild type and *Ube3a*-maternal deficient mice (8 months old). Scale bar represents 50 μm. B) Immunoblot analysis of synaptophysin and PSD95 in the straitum of $Ube3a^{m-/p+}$ mice along with wild type. Each lane represent sample from different mice.

Fig.1

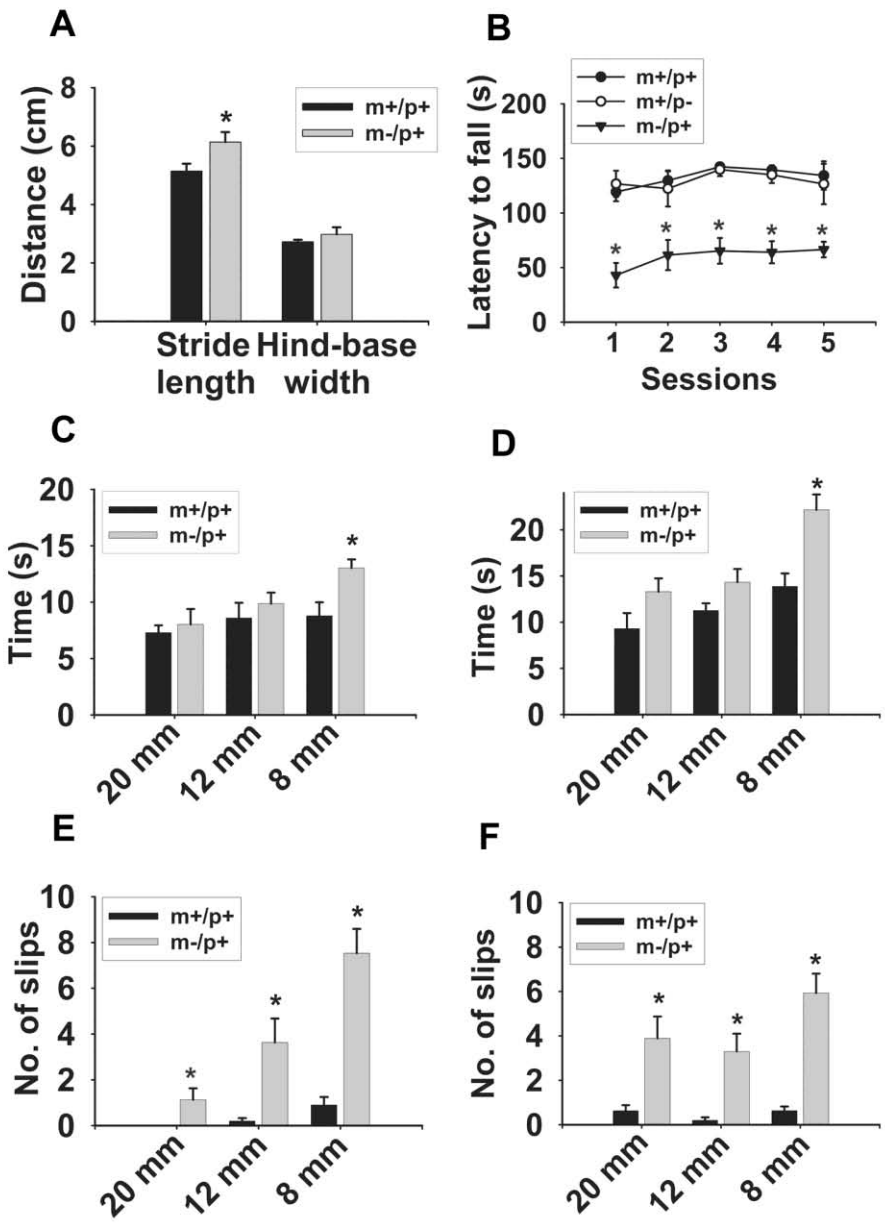

Fig.2

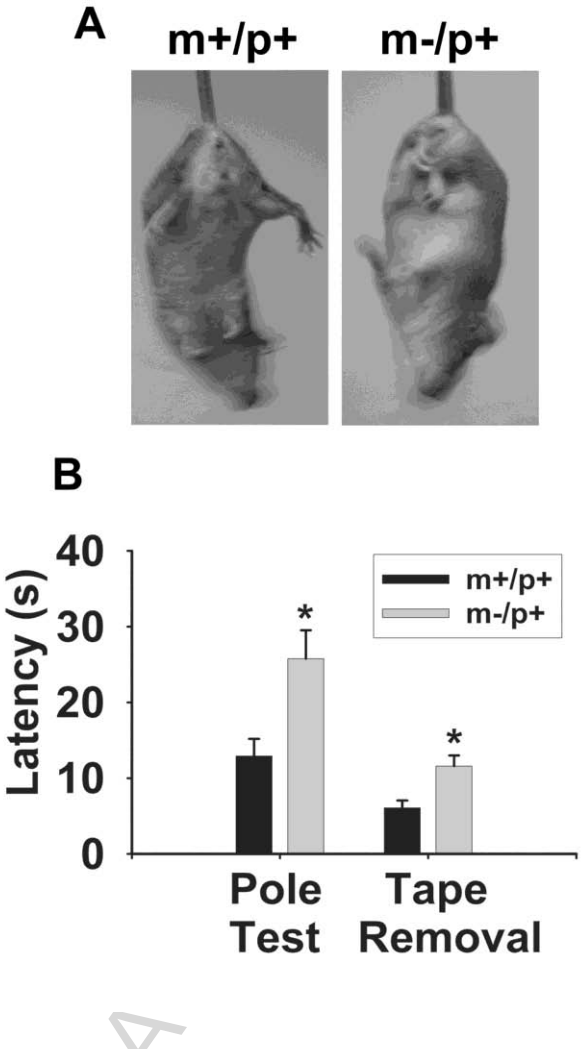

Fig.3

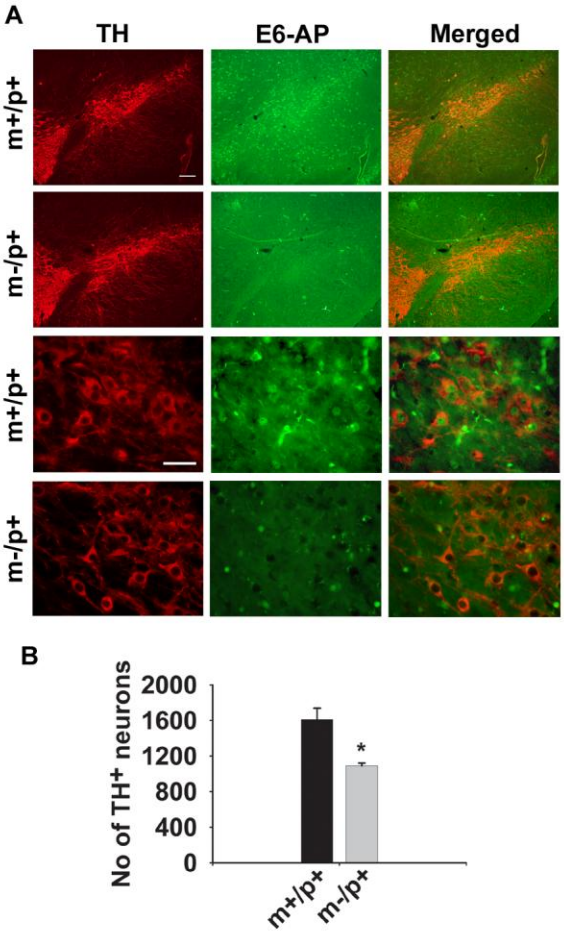

Fig.4

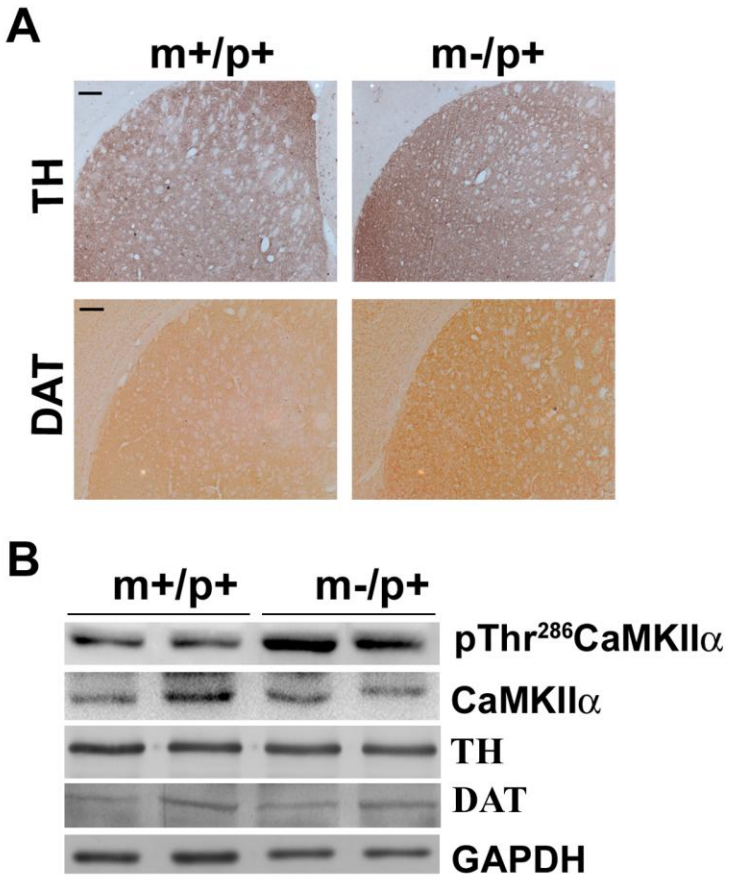

Fig.5